Supporting Information – Point defects and their impact on electrochemical performance in $Na_{0.44}MnO_2$ for sodium-ion battery cathode application

Chung-Hyok Rim, Chol-Hun Jang, Kwang-Han Kim, Chol Ryu, Chol-Jun Yu[*]

Chair of Computational Materials Design (CMD), Faculty of Materials Science, Kim Il Sung University, Pyongyang, PO Box 76, Democratic People's Republic of Korea

Table S1. Pseudopotential file name, valence electron configuration, phase, and binding energy per atom. Values in parenthesis are experimental ones [1].

Element	Pseudopotential	Configuration	Phase	E_{bind} (eV/atom)
O	O.pbe-van_ak.UPF	$2s^2 2p^4$	gas	-5.0618 (-5.12)
Li	Li.pbe-s-van_ak.UPF	$1s^2 2s^{0.95} 2p^{0.05}$	bcc	-1.9267
Na	Na.pbe-sp-van_ak.UPF	$2s^2 2p^6 3s^1$	bcc	-1.3131
K	K.pbe-sp-van.UPF	$3s^2 3p^6 4s^1$	bcc	-1.0667
Rb	rb_pbe_v1.uspp.F.UPF	$4s^2 4p^6 5s^{0.5}$	bcc	-0.9869
Mn	Mn.pbe-sp-van.UPF	$3s^2 3p^6 4s^2 3d^5$	fcc	-4.3100

[*]Corresponding author: Chol-Jun Yu, Email: cj.yu@ryongnamsan.edu.kp

Table S2. Crystal system, space group, and formation energy per O_2 of binary metal oxides, calculated by $E_{\text{form}}(M_aO_b) = [E_{\text{tot}}(M_aO_b) - aE_{\text{tot}}(M) - b/2E_{\text{tot}}(O_2)] \cdot 2/b$, where $E_{\text{tot}}(M)$ is the total energy of elementary metal per atom and $E_{\text{tot}}(O_2)$ is the total energy of isolated O_2 molecule. Experimental values are from Ref. [2].

Compound	Structure	Space group	E_{form} (eV/O_2) Cal.	Exp.
Superoxide				
LiO_2	cubic	$Fm\bar{3}m$	-0.7190	
NaO_2	cubic	$Fm\bar{3}m$	-3.2784	-2.6950
	orthorhombic	$Pnnm$	-3.3774	
	cubic	$Pa\bar{3}$	-3.3808	
	hexagonal	$R\bar{3}m$	-3.3541	
KO_2		$C12c1$	-3.4561	-2.9508
		$F4mmm$	-3.5229	
		$I4mmm$	-2.8962	
RbO_2	cubic	$I4mmm$	-3.4507	-2.8866
		$Fm\bar{3}m$	0.2057	
Peroxide				
Li_2O_2	hexagonal	$P6_3/mmc$	-5.4927	-6.5697
Na_2O_2	hexagonal	$P62m$	-4.1395	-5.2916
K_2O_2		$Cmca$	-3.8183	-5.1176
Rb_2O_2		$Immm$	-3.5259	-4.8887
Oxide				
Li_2O	cubic	$Fm\bar{3}m$	-10.3643	-12.3854
	hexagonal	$R3\bar{m}h$	-10.4348	
Na_2O	cubic	$Fm\bar{3}m$	-6.4193	-8.5801
K_2O	cubic	$Fm\bar{3}m$	-4.8546	-7.4884
Rb_2O	cubic	$Fm\bar{3}m$	-4.0629	-7.0224
MnO	cubic	$Fm\bar{3}m$	-7.2104	-7.9794
MnO_2	tetragonal	$I4m$	-5.2900	-5.3859
	tetragonal	$P4_2/mnm$	-6.3663	
	orthorhombic	$Pbnm$	-6.1844	
	orthorhombic	$Pnam$	-6.1835	
Mn_2O_3	cubic	$I213$	-7.1037	-6.6219
	cubic	IA_3	-7.0121	
	orthorhombic	$Pbca$	-7.0114	
Mn_3O_4	tetragonal	$I4_1/amd$	-7.5976	-7.1870
	orthorhombic	$Pbcm$	-6.9005	
	orthorhombic	$Pmab$	-6.9033	

Table S3. Crystal system with space group and formation energy of sodium oxides calculated using oxygen gas and sodium metal as two end materials, and corrected formation energy. $E_{\text{form}} = \frac{1}{a+b}E_{\text{tot}}(M_aO_b) - [xE_{\text{tot}}(M) - (1-x)E_{\text{tot}}(O_2)/2]$, where $x = a/(a+b)$. The correcting term E_{corr} is determined from E_{corr}^0 shown in Fig. S1 by using the relation $E_{\text{corr}} = E_{\text{corr}}^0(1-x)/2$, and then, the corrected formation energy is obtained by $E_{\text{form}}^{\text{corr}} = E_{\text{form}} - E_{\text{corr}}$.

M_aO_b	phase	a	b	$x = a/(a+b)$	E_{form} (eV)	E_{corr} (eV)	$E_{\text{form}}^{\text{corr}}$ (eV)
O_2	gas	0	2	0.0	0.0000		0.0000
NaO_3	orthorhombic ($Imm2$)	1	3	1/4	-0.6816		-0.6816
NaO_2	cubic ($Fm\bar{3}m$)	1	2	1/3	-1.1270	-0.2025	-0.9245
	orthorhombic ($Pnnm$)				-1.0928		-0.8904
	cubic ($P\bar{a}3$)				-1.1180		-0.9156
	hexagonal ($R\bar{3}m$)				-1.1258		-0.9233
Na_2O_2	hexagonal ($P\bar{6}2m$)	2	2	1/2	-1.0349	0.3057	-1.3406
Na_2O	cubic ($Fm\bar{3}m$)	2	1	2/3	-1.0699	0.2038	-1.2737
Na	cubic (bcc)	1	0	1.0	0.0000		0.0000

Table S4. Crystal system with space group, total energy, and formation energy of titanium oxides calculated using oxygen gas and titanium metal as two end materials. $E_{\text{form}} = \frac{1}{a+b}E_{\text{tot}}(\text{M}_a\text{O}_b) - [xE_{\text{tot}}(\text{M}) - (1-x)E_{\text{tot}}(\text{O}_2)/2]$, where $x = a/(a+b)$.

M_aO_b	phase	a	b	$x = a/(a+b)$	E_{form} (eV)
O_2	gas	0	2	0.0	0.0000
Mn_2O_7	monoclinic ($P2_1/c$)	2	7	0.2222	-0.6230
MnO_2	monoclinic ($C12/m1$)	1	2	0.3333	-1.7233
	tetragonal ($I4m$)	1	2	0.3333	-1.5574
	tetragonal ($P42mnm$)	1	2	0.3333	-1.5571
	orthorhombic ($Pbnm$)	1	2	0.3333	-1.6732
Mn_5O_8	monoclinic ($C12/m1$)	5	8	0.3846	-1.9057
Mn_2O_3	orthorhombic ($Pbca$)	2	3	0.4000	-2.1311
	cubic (IA_3)	2	3	0.4000	-2.1044
	cubic ($I213$)	2	3	0.4000	-2.1041
Mn_3O_4	tetragonal ($I4_1/amd$)	3	4	0.4286	-2.1707
	orthorhombic ($Pbcm$)	3	4	0.4286	-2.0429
	orthorhombic ($Pmab$)	3	4	0.4286	-2.0437
MnO	cubic ($Fm\bar{3}m$)	1	1	0.5000	-1.9087
Mn	cubic (fcc)	1	0	1.0	0.0000

Table S5. Space group, elementary formation energy per atom from bcc Na metal, fcc Mn metal and O_2 gas (E_f^{el}), and formation reaction and energy (E_f^{bi}) from binary oxides for Na–Mn–O system.

Compound	Space group	E_f^{el} (eV)	Binary oxides	
			Reaction	E_f^{bi} (eV)
$\text{Na}_{14}\text{Mn}_2\text{O}_9$	$P3$	-1.3679	$7\text{Na}_2\text{O} + 2\text{MnO}$	-0.1459
Na_5MnO_4	$P2_1m$	-1.5158	$5/2\text{Na}_2\text{O} + 1/2\text{Mn}_2\text{O}_3$	-0.1806
$\text{Na}_4\text{Mn}_2\text{O}_5$	$Fddd$	-1.7528	$2\text{Na}_2\text{O} + \text{Mn}_2\text{O}_3$	-0.2005
$\text{Na}_2\text{Mn}_3\text{O}_7$	$P1$	-1.8924	$2\text{NaO}_2 + 3\text{MnO}$	-0.3356
Na_2MnO_4	$P63mc$	-1.3423	$\text{NaO}_2 + \text{NaMnO}_2$	-0.5142
NaMn_2O_4	$Pnam$	-2.1028	$\text{NaO}_2 + 2\text{MnO}$	-0.4797
			$1/2\text{Na}_2\text{O}_2 + \text{Mn}_2\text{O}_3$	-0.2849
NaMnO_2	$C2m$	-2.1365	$1/2\text{Na}_2\text{O}_2 + \text{MnO}$	-0.6086
			$1/2\text{N}_2\text{O} + 1/2\text{Mn}_2\text{O}_3$	-0.4033
$\text{NaMn}_7\text{O}_{12}$	$I2m$	-2.2161		

Table S6. Oxygen chemical potential $\Delta\mu_O$ (T, p) as increasing temperature T from 300 K to 1500 K with the experimental data of entropy $S°$, enthalpy difference $H°(T) - H°(Tr)$, and $H°(Tr) - H°(0) = 0.0899$ eV available from Ref. [2], where the reference temperature is $Tr = 298.15$ K. Here, $\Delta\mu_O$ (T, p) is evaluated at the pressure values of $p = p_\circ = 1$ atm and $p = 0.2$ atm, respectively.

T		$S°$	$H°(T) - H°(Tr)$	$TS°$	$\Delta\mu_O$ $(T, p_\circ)$		$\frac{1}{2}k_B T \ln(p/p_\circ)$	$\Delta\mu_O$ (T, p)
(°C)	(K)	(J/mol·K)	(kJ/mol)	(kJ/mol)	(kJ/mol)	(eV)	(eV)	(eV)
25	298.15	205.148	0.000	61.1649	−26.2424	−0.2718	−0.0207	−0.2925
26.85	300	205.330	0.054	61.5990	−26.4325	−0.2738	−0.0208	−0.2946
126.85	400	213.873	3.026	85.5492	−36.9216	−0.3824	−0.0277	−0.4102
226.85	500	220.695	6.085	110.3475	−47.7913	−0.4950	−0.0347	−0.5297
326.85	600	226.454	9.245	135.8724	−58.9737	−0.6108	−0.0416	−0.6524
426.85	700	231.470	12.500	162.0290	−70.4245	−0.7294	−0.0485	−0.7780
526.85	800	235.925	15.838	188.7400	−82.1110	−0.8505	−0.0555	−0.9059
626.85	900	239.937	19.244	215.9433	−94.0097	−0.9737	−0.0624	−1.0361
726.85	1000	243.585	22.707	243.5850	−106.0990	−1.0989	−0.0693	−1.1683
826.85	1100	246.930	26.217	271.6230	−118.3630	−1.2259	−0.0763	−1.3022
926.85	1200	250.019	29.768	300.0228	−130.7874	−1.3546	−0.0832	−1.4378
1026.85	1300	252.888	33.352	328.7544	−143.3612	−1.4849	−0.0901	−1.5750
1126.85	1400	255.568	36.968	357.7952	−156.0736	−1.6165	−0.0971	−1.7136
1226.85	1500	258.081	40.611	387.1215	−168.9153	−1.7495	−0.1040	−1.8536

Table S7. Oxygen chemical potential $\Delta\mu_O$ (T, p) as decreasing oxygen partial pressure p from 10^9 atm to 10^{-9} atm at temperatures of $T = 1100$ K and 700 K.

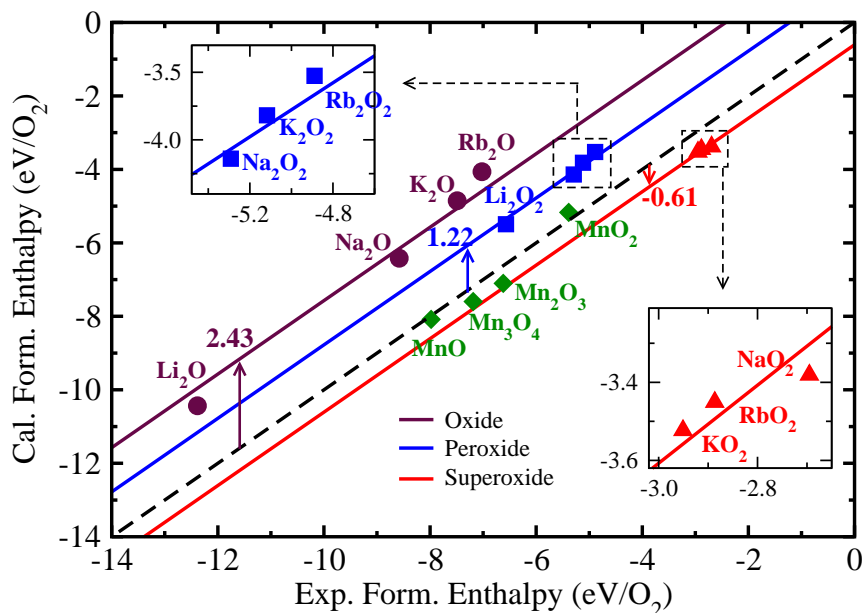| p		$\frac{1}{2}k_B T \ln(p/p_\circ)$	$\Delta\mu_O$ (T, p) (eV)	
(Pa)	(atm)	(eV)	1100 K	700 K
10^{14}	10^9	0.9822	−0.2438	0.2528
10^{11}	10^6	0.6548	−0.5711	−0.0746
10^8	10^3	0.3274	−0.8985	−0.4020
10^5	10^0	0.0000	−1.2259	−0.7294
10^2	10^{-3}	−0.3274	−1.5533	−1.0568
10^{-1}	10^{-6}	−0.6548	−1.8807	−1.3842
10^{-4}	10^{-9}	−0.9822	−2.2081	−1.7116

Figure S1. The calculated formation enthalpy versus experimental formation enthalpy for alkali metal oxides and manganese oxides. For alkali metal oxides, systematic differences are found, giving the correction energy for oxide formation energy $E_{\text{oxd}}^{\text{cor}} = -0.61$, 1.22, and 2.43 eV per O_2 for superoxide, peroxide and oxide, respectively.
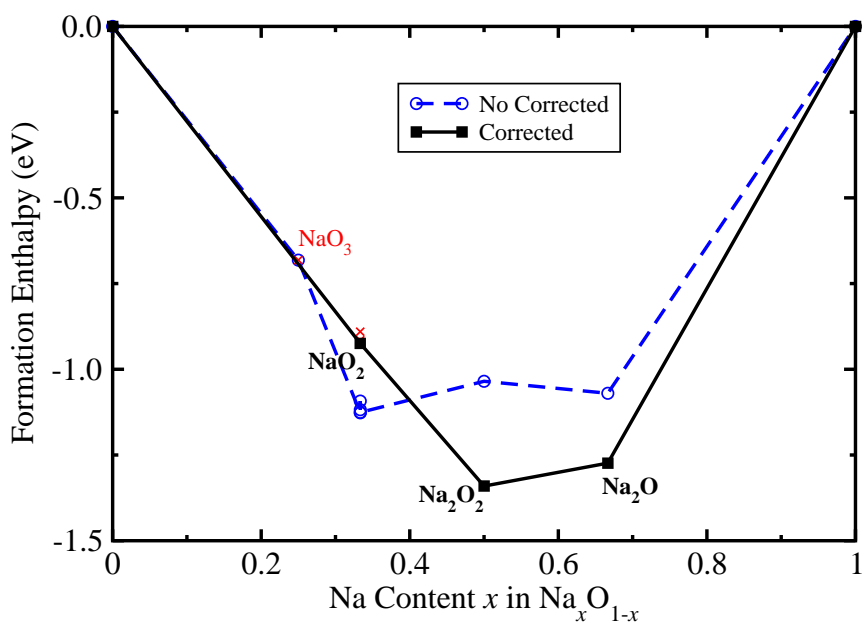

Figure S2. Convex hull plot of formation energies of the binary Na–O system. Red-colored dashed line is for the original formation energies, and black-colored solid line is for the formation energies corrected with $E_{\text{oxd}}^{\text{cor}}$.
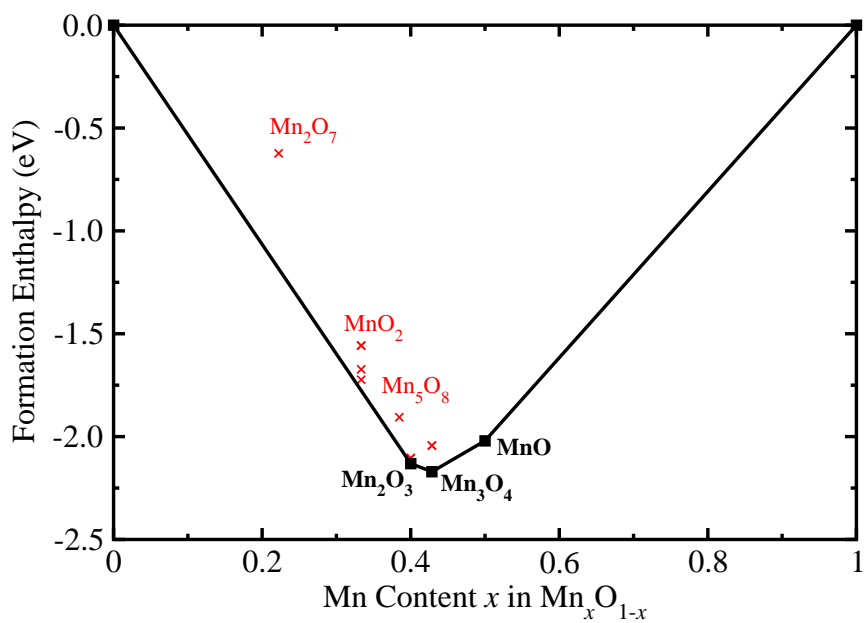
Figure S3. Convex hull plot of formation energies of the binary Mn–O system.
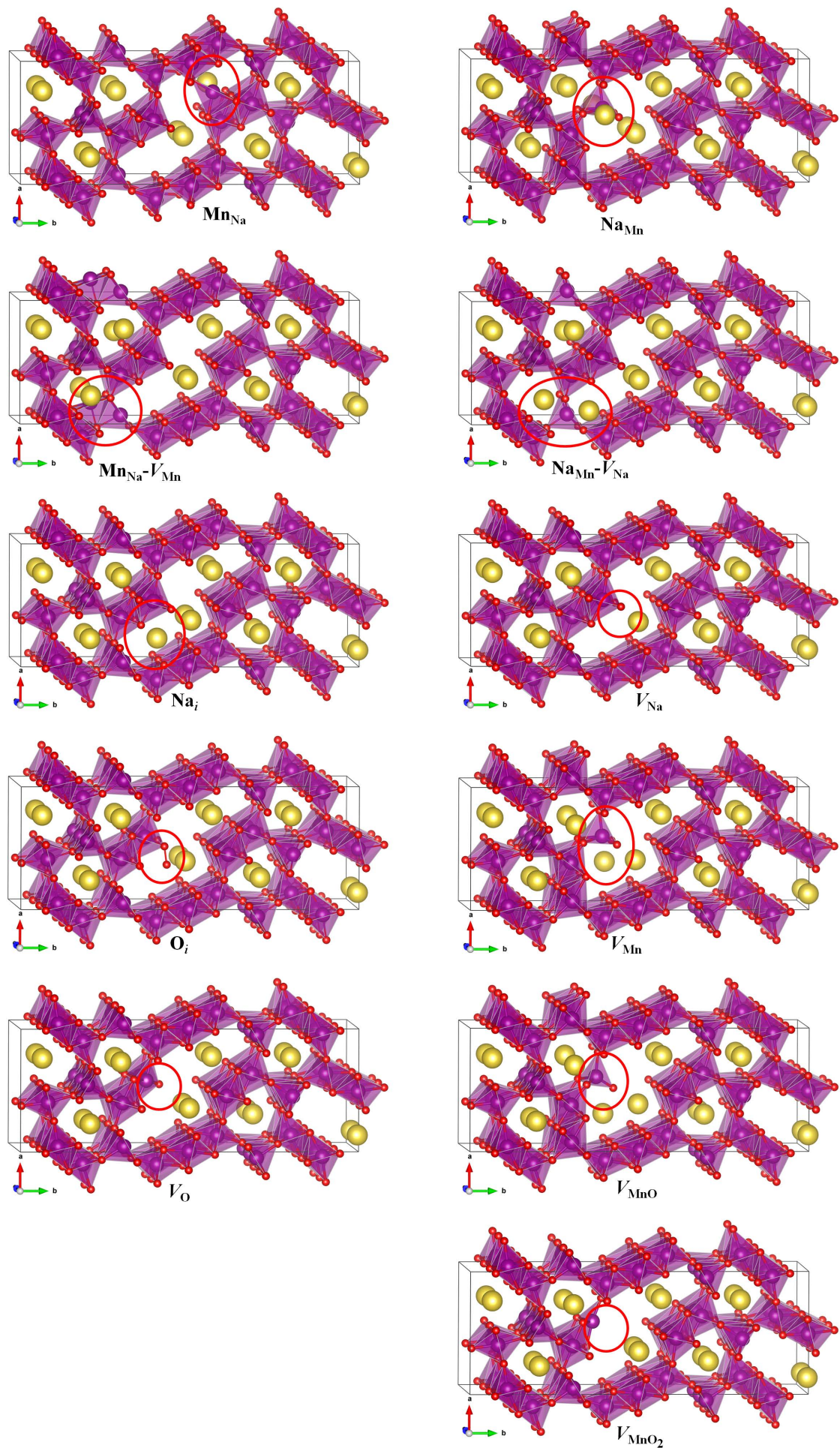
Figure S4. Polyhedral view of $(1 \times 1 \times 2)$ supercell containing intrinsic point defects in $Na_4Mn_9O_{18}$.
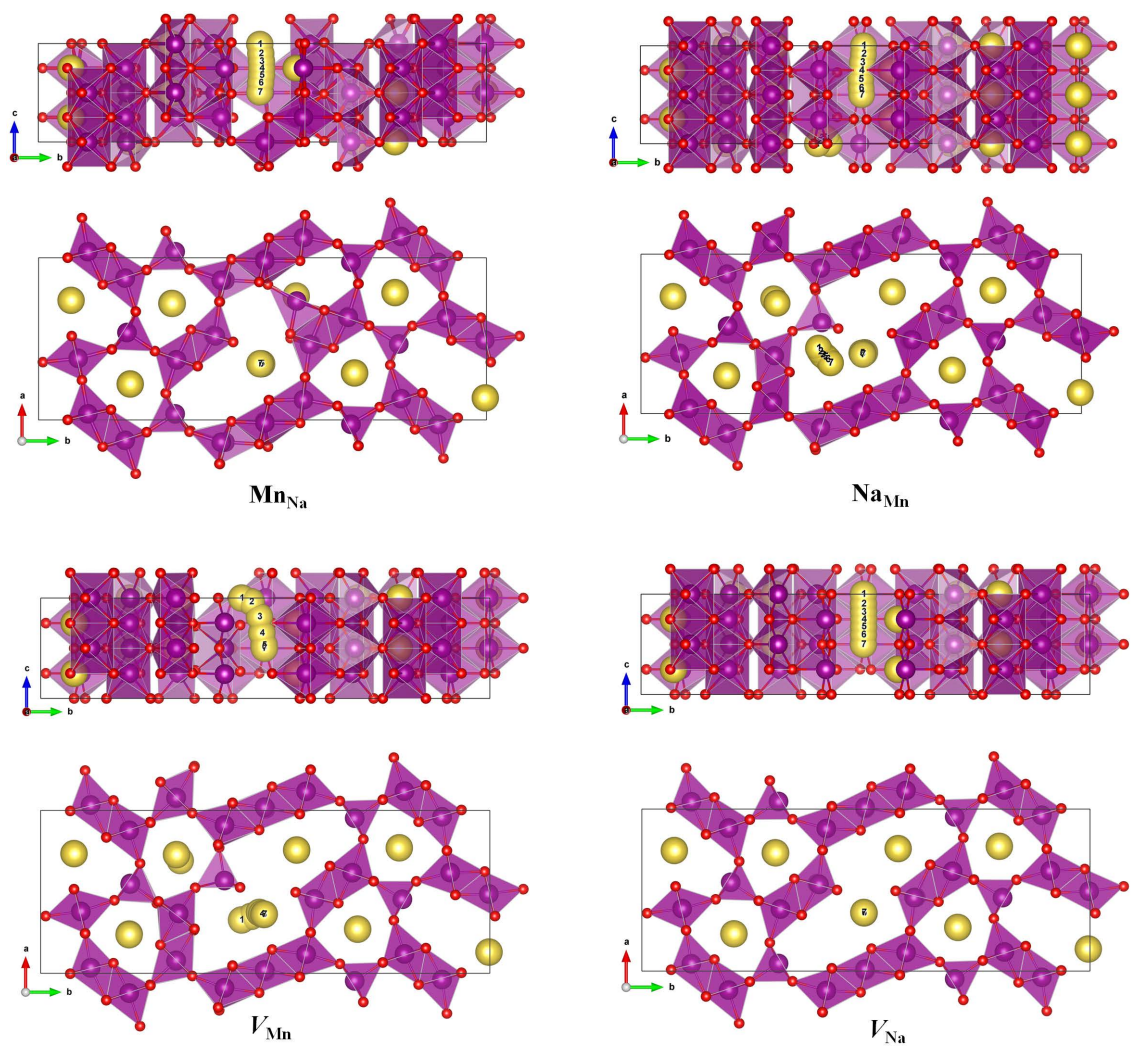
Figure S5. Polyhedral view for Na ion migration in $(1 \times 1 \times 2)$ supercell containing intrinsic point defects, such as Mn_{Na}, Na_{Mn}, V_{Mn} and V_{Na}, in $Na_4Mn_9O_{18}$.
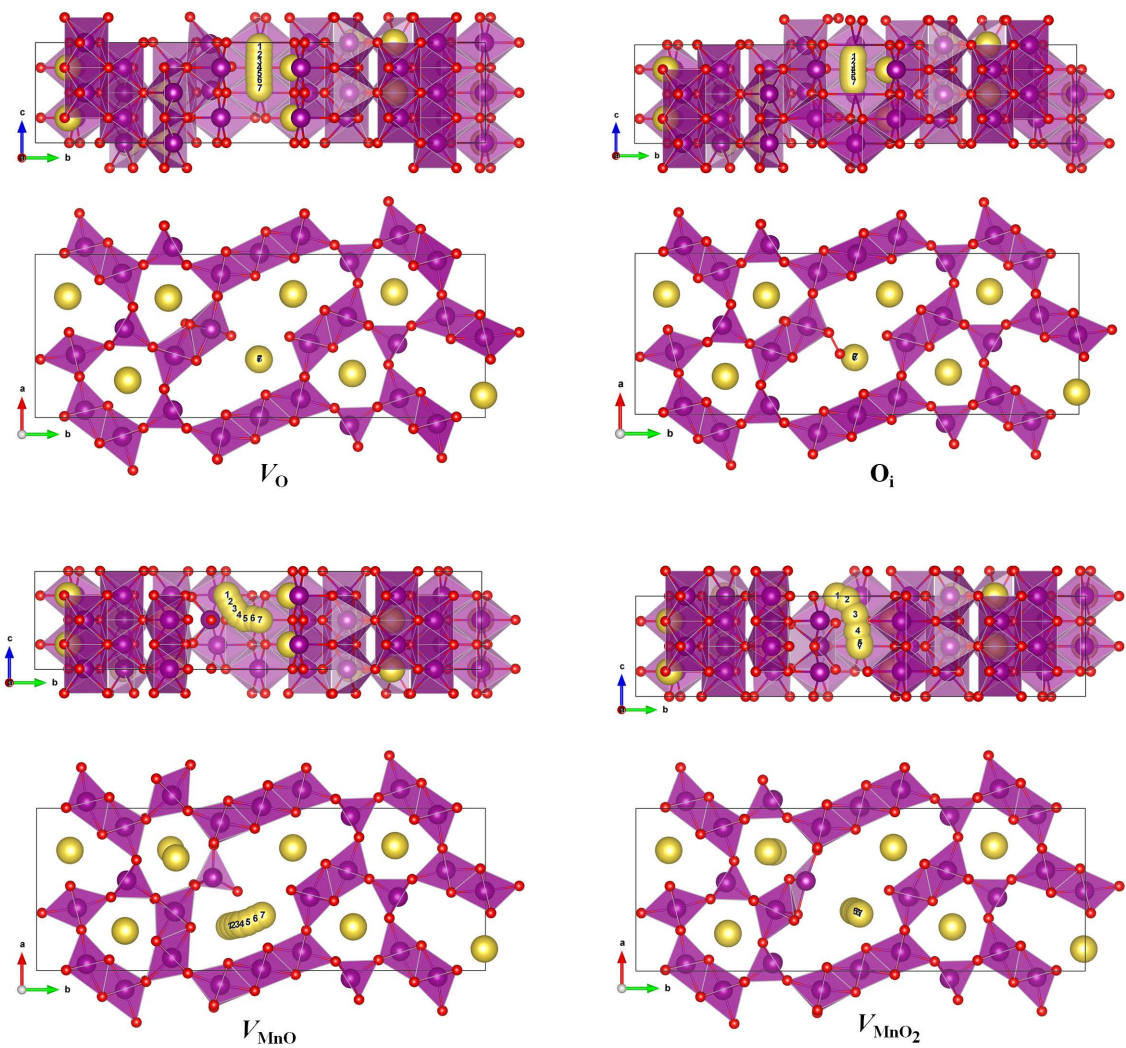
Figure S6. Polyhedral view for Na ion migration in (1×1×2) supercell containing intrinsic point defects and defect complexes, such as V_O, O_i, V_{MnO} and V_{MnO_2}, in $Na_4Mn_9O_{18}$.

References

[1] M. W. Chase, Jr., *NIST-JANAF Themochemical Tables*, Fourth Edition (J. Phys. Chem. Ref. Data, Monograph 9, 1998) pp. 11951.

[2] *CRC Handbook of Chemistry and Physics*, Internet Version, D. R. Lide Ed.; CRC Press: http://www.hbcpnetbase.com, Boca Raton, FL (2005).